Reaction of Butanes on Na,H−Y Zeolites and H-Mordenites

Jozsef Engelhardt

Central Research Institute for Chemistry of the Hungarian Academy of Sciences, H-1525 Budapest, P.O. Box 17, Hungary
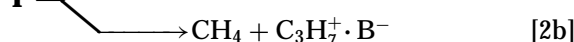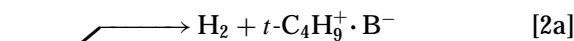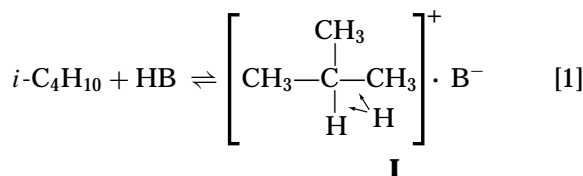
The reaction chemistry for the conversion of isobutane and *n*-butane on H-mordenites was compared with that on Na,H−Y zeolites in continuous flow experiments. The close resemblance of the product distribution as a function of conversion suggests that identical mechanism for conversion is effective on both types of zeolites. Hydrogen and methane from isobutane and in addition ethane and ethylene from *n*-butane were expected to be formed in chain initiation processes, while propene and butenes were expected to be formed in chain termination processes. The major products, alkanes, are produced in chain carrying hydride and methyl transfer. A rate of initiation approximately 10-fold higher than with mordenites having stronger Brønsted acid sites is required to reach identical conversion with Y-zeolites. The yield of individual products on zeolites with identical structure and at identical temperature was almost independent of the Si/Al ratio or the Na$^+$ content of zeolites but depended on the conversion; at identical conversion the chain length on zeolites with different activity was similar. © 1996 Academic Press, Inc.
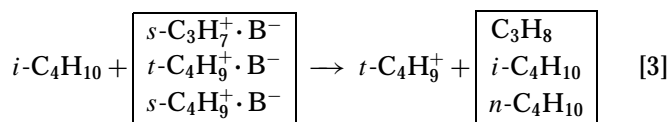
INTRODUCTION

The cracking and isomerization of various alkanes have been used for many years to test the performance of acid catalysts. Recent studies have revealed that conversion of isobutane giving few products is a sensitive probe reaction (1–14).

It has been shown by Hall and co-workers (4–11) that on acid catalysts the reaction of isobutane is initiated by protonation of C−H or C−C bonds on Brønsted acid sites. The first formed pentacoordinated carbonium ions decompose into carbenium ions (*t*-butyl and propyl) and the products of the initiation reactions, viz. hydrogen and methane

$$i\text{-}C_4H_{10} + HB \rightleftharpoons \left[\begin{array}{c} CH_3 \\ | \\ CH_3{-}C{-}CH_3 \\ | \\ H \diagdown H \end{array} \right]^+ \cdot B^- \qquad [1]$$

$$\mathbf{I}$$

$$\mathbf{I} \nearrow \begin{array}{l} \rightarrow H_2 + t\text{-}C_4H_9^+ \cdot B^- \qquad [2a] \\ \\ \rightarrow CH_4 + C_3H_7^+ \cdot B^- \qquad [2b] \end{array}$$
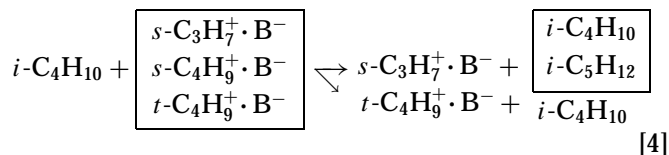
where HB is a Brønsted acid site of the zeolite and **I** is the three center two electron bonded pentacoordinated carbonium ion described by Olah and co-workers (15–17).

Once the initial carbenium ions are formed, they can undergo isomerization, decompose to alkenes, or take part in other reactions. Wojciechowski and co-workers (18) proposed that even at low conversion, bimolecular chain processes take place between feed molecules and various carbenium ions. They classified these processes into "hydride transfer" and "dimerization cracking," both leading to the formation of a gas phase alkane and a new carbenium ion. According to Marczewski (19), like original Brønsted sites, carbenium ions can attack C−H and C−C bonds of the feed molecule to form pentacoordinated transition complexes, which decompose *via* routes leading to hydride or alkyl transfer (the latter being identical with Wojciechowski's "dimerization cracking"). In hydride transfer the carbon number of alkane is identical to that of the original carbenium ion, while in alkyl transfer it is smaller or larger. Thus, by considering the carbenium ion isomers from isobutane

$$i\text{-}C_4H_{10} + \boxed{\begin{array}{c} s\text{-}C_3H_7^+ \cdot B^- \\ t\text{-}C_4H_9^+ \cdot B^- \\ s\text{-}C_4H_9^+ \cdot B^- \end{array}} \longrightarrow t\text{-}C_4H_9^+ + \boxed{\begin{array}{c} C_3H_8 \\ i\text{-}C_4H_{10} \\ n\text{-}C_4H_{10} \end{array}} \qquad [3]$$

where the second reaction is degenerate with actual hydride transfer. On the other route,

$$i\text{-}C_4H_{10} + \boxed{\begin{array}{c} s\text{-}C_3H_7^+ \cdot B^- \\ s\text{-}C_4H_9^+ \cdot B^- \\ t\text{-}C_4H_9^+ \cdot B^- \end{array}} \searrow \begin{array}{c} s\text{-}C_3H_7^+ \cdot B^- \\ t\text{-}C_4H_9^+ \cdot B^- \end{array} + \boxed{\begin{array}{c} i\text{-}C_4H_{10} \\ i\text{-}C_5H_{12} \\ i\text{-}C_4H_{10} \end{array}} \qquad [4]$$

where the first and last reactions are degenerate with actual methyl transfer.

Chain termination occurs by deprotonation of carbenium ions resulting in formation of alkenes and restoration of Brønsted acid sites. The equilibrium between surface bound carbenium ion and gas phase alkene,
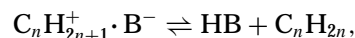
$$C_nH_{2n+1}^+ \cdot B^- \rightleftharpoons HB + C_nH_{2n},$$

TABLE 1

Description of the Catalysts

Catalysts	Chemical analysis (wt%)			Al_T/g^a $(\times 10^{-20})$	Al_F/g^a $(\times 10^{-20})$	Si/Al $(F)^a$	Pore vol.^{a}	$-H_0^b$	Source
	SiO_2	Al_2O_3	Na_2O						
LZ–210(6)[2.0]	77.2	20.8	2.0	22.8	22.8	3.4	0.33	10.0	UOP
LZ–210(6)[0.45]	78.4	21.1	0.45	23.2	22.8	3.4	0.33	10.5	UOP
LZ–210(6)[0.1]	78.8	21.1	0.1	23.3	22.8	3.4	0.33	12.0	UOP
LZ–210(9)[0.1]	84.0	15.9	0.1	16.8	17.6	4.7	0.33	11.0	UOP
LZ–210(12)[0.46]	86.9	12.7	0.46	14.8	14.6	6.0	0.33	10.0	UOP
LZ–210(12)[0.1]	87.3	12.7	0.1	14.9	14.6	6.0	0.33	12.0	UOP
LZ–Y82	75.7	24.1	0.46	28.3	15.8	5.2	0.32	12.0	UOP
JRC–Z–HM10	85.3	14.6	0.1	17.3	17.0	4.9	0.18	12.4	CSJ^c
JRC–Z–HM15	89.7	10.2	0.1	12.0	12.0	7.5	0.18	—	CSJ
JRC–Z–HM20	92.1	7.8	0.1	9.2	9.2	10.0	0.18	—	CSJ
LZ–M8	90.9	9.1	0.1	10.6	10.6	8.9	0.18	12.4	UOP

^{a} Al_T/g is the total Al per gram determined by chemical analysis; Al_F/g is the framework Al from ^{29}Si MASNMR; Si/Al (F) is the ratio calculated from NMR data; Pore vol. is given in cm^3/g and was calculated from BET measurements.

^{b} From Ref. (12). $-H_0$ values of the acid sites of the catalysts were deduced from the spectral shifts of adsorbed 4-nitrotoluene and 4-nitrofluorobenzene on contact with the catalyst; these bases were not protonated by these zeolites.

^{c} Catalysis Society of Japan.

is a function of temperature, strength of acid site, and size (character) of the carbenium ion. Moreover, released alkenes can be protonated more easily to form carbenium ion on free Brønsted sites than feed molecules.

It was found by Umansky *et al.* (12) that the Brønsted acid sites of NaH–Y zeolites differed from those of H-mordenites. The acid strength of NaH–Y zeolites varied from $-H_0 = 10$ to 12, equivalent to sulfuric acid of 89–100% concentration, while that of H-mordenite is equal to $-H_0 = 12.4$, stronger than concentrated sulfuric acid, equivalent to fumic acid of 25% concentration (see Table 1).

In the present work the reactions of isobutane on H–Y zeolites are compared with those on the more acidic H-mordenites.

EXPERIMENTAL

Catalysts. The catalysts used and their properties are listed in Table 1. LZ–210(6), LZ–210(9) and LZ–210(12) were silicon enriched Y-zeolites furnished by UOP. They were treated at 90°C with 1.0 *M* ammonium acetate to reduce their sodium content and then after filtering were dried at 120°C. LZ–Y82 was an ultrastable Y-zeolite obtained from the same source and was used without modification. Catalysts JRC–Z–HM10, HM15, and HM20 were Japan Reference Catalysts and LZ–M8 was another UOP product. These mordenites were used without modification.

Before the experiments, the catalysts were given a *standard pretreatment*. The powder was pressed into pellets without binder, crushed and sieved. A few grams of the 20–40 mesh fraction (0.425–0.85 mm) were heated in step-

wise fashion in an open quartz crucible to 500°C and held there for 5 h. After being covered with a lid, the catalysts were cooled and 400-mg aliquots were packed into a quartz U-tube reactor between quartz wool plugs. The reactor was heated in a stepwise fashion and held overnight at 500°C in flowing dry O_2. Finally the catalyst was flushed with dried prepurified N_2 and cooled to the preselected reaction temperature.

Apparatus and procedures. The catalytic tests were carried out at atmospheric pressure in a continuous flow reactor system. The reactor was held at temperatures constant to ±0.2°C inside an electrically heated furnace. The temperature was monitored by a thermocouple placed externally near the center of the about 2-cm-long catalyst bed.

The reactants were isobutane (containing 0.04% propane and 0.2% *n*-butane) and *n*-butane (containing 0.06% isobutane); both were Matheson instrument purity grade. These gases were diluted with N_2 (Matheson, prepurified grade) in 1 : 9 ratio by using a Brooks dual channel mass flow controller unit. In some experiments N_2 containing 0.1% ethylene, propene, or *i*-butene (Matheson gas mixtures) was used for dilution instead of pure N_2. In experiments where the temperature and the partial pressure of reactant were kept constant while the feed rate was varied, preprepared mixtures containing isobutane or *n*-butane in 90% N_2 were used.

The reaction was started by switching the reactor from nitrogen to the reactant mixture stream. The effluent gas from reactor was sampled and analyzed by on-line GC. Two GCs were connected parallel, and N_2 was used as carrier gas.

TABLE 2

TOF of Isobutane Conversion on HY Zeolites at 370°C[a]

Catalyst	LZ–210(6)[0.1]	LZ–210(9)[0.1]	LZ–210(12)[0.1]	LZ–Y82
H_2	2.0	2.0	3.0	3.5
CH_4	1.5	2.5	3.0	4.0
C_2H_6	0.0	0.0	0.0	0.0
C_2H_4	0.0	0.0	0.0	0.0
C_3H_8	1.5	3.2	5.0	7.4
C_3H_6	0.5	0.5	0.7	1.0
$n\text{-}C_4H_{10}$	6.5	18.9	27.3	39.7
$i\text{-}C_4H_8$	1.2	1.7	2.0	2.7
$n\text{-}C_4H_8$	0.0	0.0	0.0	0.0
$i\text{-}C_5H_{12}$	0.0	2.0	3.2	4.7
$n\text{-}C_5H_{12}$	0.0	0.0	0.0	0.0
$H_2 + CH_4$	3.5	4.5	6.0	7.5
Σ_3^5 alkanes	8.0	24.1	35.5	51.9
Conv.$(A)^b$	11.5	28.6	41.5	59.4
Conv.$(B)^c$	9.7	26.3	38.7	55.8
$C_4/(C_3 + C_5)^d$	4.3	3.6	3.3	3.3
$C_3/C_5{}^d$	—	1.6	1.6	1.6
% initiation^e	31.6	16.0	16.8	12.6
Chain length^f	2.3	5.4	6.0	6.9
% conv.(B)	0.3	0.7	0.8	0.7

^{a} TOF is given as 10^{-6} molec. $Al_F^{-1}s^{-1}$; 400 mg of catalyst was used; $F/W = 1.1 \times 10^{-5}$ mol $g^{-1}s^{-1}$.

^{b} Conversion$(A) = (H_2 + CH_4) + \Sigma_3^5$ alkanes.

^{c} Conversion$(B) = 1/4 \Sigma_1^5 jC_i$, where j is the number of carbon atoms in each of the i products.

^{d} Ratio of alkanes.

^{e} % initiation reaction $= [(H_2 + CH_4)/Conv.(A)] \times 100$.

^{f} Σ_3^5 alkanes/$(H_2 + CH_4)$; i.e., the number of isobutane molecules reacted by hydride or alkyde transfer for every chain initiated by Brønsted acid sites.

In the first, hydrogen was separated and determined on 5A molecular sieve column at 0°C using a thermal conductivity detector. In the second, hydrocarbons were separated at 0°C over two packings in series (dibenzylamine and propylene carbonate on chromosorb) and determined using a flame ionization detector.

Treatment of the data. The composition of the products was calculated as the mole fraction (X_i) of the total product after correction was made for the impurities in the feed. Differential reaction rates were calculated at low conversion as $C_i = X_i(F/W)$, where (F/W) is the entering reactant in moles per gram per second. These rates were expressed as turnover frequencies (TOF) by converting the data to molec. s^{-1} Al_F^{-1}. Per cent conversions were expressed as $100 \times$ Conversion$(B) \times (F/W)^{-1}$. Here Conversion$(B) = 1/4\Sigma_1^5 jC_i$. Here j is the number of carbon atoms in each of the i products. Yields were calculated as moles of the ith product formed per 100 moles of reactant passed. Conversions were varied by changing F/W on constant weight of catalyst.

RESULTS

Reactions of isobutane. The TOFs for product formation in the steady state conversion of isobutane at 370°C over four different H−Y and at 300°C over four different H−M zeolites are presented in Tables 2 and 3, respectively. A more direct comparison of the two types of zeolites was not possible: below 350°C, conversion on H−Y zeolites was almost unobservable; above 300°C, steady-state conversions over mordenites could not be attained due to the extensive coke formation.

Under the conditions selected, *n*-butane, propane, and (especially on mordenites) pentanes were the chief products. The contribution of $(H_2 + CH_4)$ initiation products to the total product decreased with increasing Si/Al ratio on both types of zeolite and varied between 13 and 32% over H−Y and between 0.4 and 1.5% over mordenites. Conversely, the TOFs for alkane formation increased with increasing Si/Al ratio. This stemmed from the increasing contribution of carbenium ion chain reactions with increasing Si/Al ratio and from their much larger contribution over

TABLE 3

TOF of Isobutane Conversion on H-Mordenites at 300°C[a]

Catalyst	JRC–Z–HM10	JRC–Z–HM15	JRC–Z–HM20	LZ–M8
H_2	2.0	3.5	3.2	5.7
CH_4	1.5	2.5	2.5	8.9
C_2H_6	0.0	0.2	0.2	0.0
C_2H_4	1.0	3.0	3.5	1.7
C_3H_8	97.5	312.7	409.3	141.7
C_3H_6	0.7	1.5	1.7	3.5
$n\text{-}C_4H_{10}$	178.9	575.8	801.9	284.9
$i\text{-}C_4H_8$	1.7	2.5	3.7	5.2
$n\text{-}C_4H_8$	0.0	0.0	1.0	0.0
$i\text{-}C_5H_{12}$	79.4	220.4	311.0	151.1
$n\text{-}C_5H_{12}$	10.9	49.4	63.0	9.2
$H_2 + CH_4$	3.5	6.0	5.7	14.6
Σ_3^5 alkanes	366.7	1158.3	1585.2	586.9
Conv.$(A)^b$	370.2	1164.3	1590.9	601.5
Conv.$(B)^c$	368.3	1154.6	1583.9	602.8
$C_4/(C_3 + C_5)^d$	1.0	1.0	1.0	1.1
$C_3/C_5{}^d$	0.9	1.2	1.1	0.9
% initiation^e	0.9	0.5	0.4	1.4
Chain length^f	105.0	193.0	278.0	40.0
% conv.(B)	4.2	9.0	9.5	3.8

^{a} TOF is given as 10^{-6} molec. $Al_F^{-1}s^{-1}$; 400 mg of catalyst was used; $F/W = 1.1 \times 10^{-5}$ mol $g^{-1}s^{-1}$.

^{b} Conversion$(A) = (H_2 + CH_4) + \Sigma_3^5$ alkanes.

^{c} Conversion$(B) = 1/4 \Sigma_1^5 jC_i$, where j is the number of carbon atoms in each of the i products.

^{d} Ratio of alkanes.

^{e} % initiation reaction $= [(H_2 + CH_4)/Conv.(A)] \times 100$.

^{f} Σ_3^5 alkanes/$(H_2 + CH_4)$; i.e., the number of isobutane molecules reacted by hydride or alkyde transfer for every chain initiated by Brønsted acid sites.
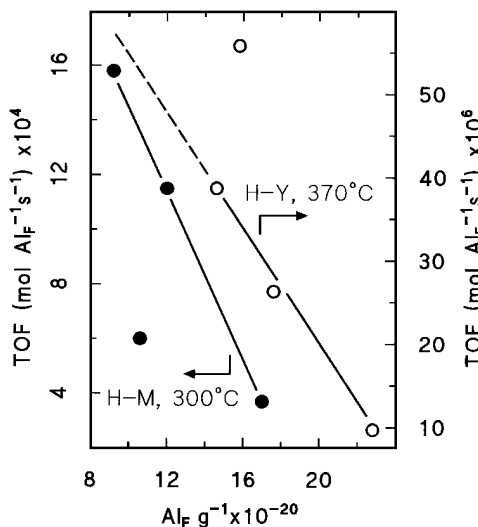
FIG. 1. Isobutane conversion (TOF) over H–Y zeolites at 370°C (○) and on H-mordenites at 300°C (●) as a function of framework Al content; 400 mg of catalyst was used; F/W was 1.1×10^{-5} moles $g^{-1}s^{-1}$.

mordenites. The TOF of overall conversion [Conv. (B)] increased linearly with decreasing framework Al content within a series of related catalysts (Fig. 1). Results on different preparations (LZ–Y82 and LZ–M8) do not obey this rule.

Experiments with varying feed rate (F/W) of isobutane and constant weight (400 mg) of catalysts were carried out at 370°C on H–Y and at 250°C over H–M zeolites. Data are plotted as yields of individual products vs total conversion in Figs. 2 and 3 for Y-zeolites and in Fig. 4 for mordenites. *Significantly, in each case the experimental points*
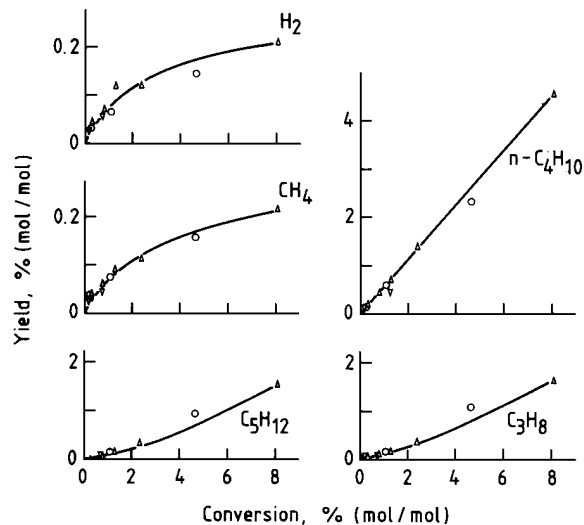

FIG. 3. Yield of individual products (moles of product per 100 moles passed) as a function of the total conversion of isobutane on Na, H–Y zeolites at 370°C; (△) LZ–210(6)[0.1], (○) LZ–210(6)[0.45], (▽) LZ–210(6)[2.0]; 400 mg of catalyst was used; F/W was varied between 1.1×10^{-5} and 1.8×10^{-6} moles $g^{-1}s^{-1}$ from the higher to the lower values.

for the different catalysts all fell on the same lines. These were nearly linear for alkanes, whereas the plots for hydrogen and methane tended to level off or approach a low constant slope after the initial sharp increases. The shape of the curves for butenes and propene on Y-zeolites followed the shape of those for hydrogen and methane. Only traces of alkenes were found in the products on mordenites. Note that a nearly 10-fold larger yield of initiation products ($H_2 + CH_4$) was required for the Y-zeolites

FIG. 2. Yield of individual products (moles of products per 100 moles passed) as a function of the total conversion of isobutane on H–Y zeolites at 370°C; (△) LZ–210(6)[0.1], (▢) LZ–210(9)[0.1], (▽) LZ–210(12)[0.1], (○) LZ–Y82; 400 mg of catalyst was used; F/W was varied between 1.1×10^{-5} and 1.8×10^{-6} moles $g^{-1}s^{-1}$ from the higher to the lower values.
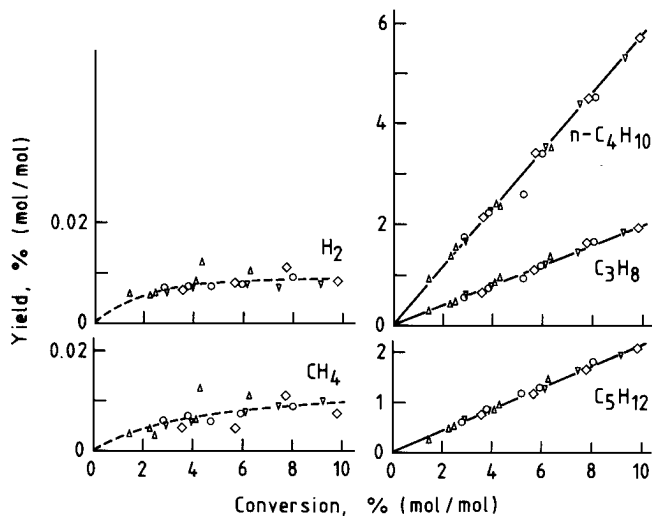

FIG. 4. Yield of individual products (moles of product per 100 moles passed) as a function of the total conversion of isobutane on H-mordenites at 250°C; (△) JRC–Z–HM10, (◇) JRC–Z–HM15, (▽) JRC–Z–HM20, (○) LZ–M8; 400 mg of catalyst was used; F/W was varied between 1.1×10^{-5} and 1.8×10^{-6} moles $g^{-1}s^{-1}$ from the higher to the lower values.

to maintain yields of the major products comparable with those on mordenites. This required that the temperature be raised by $120°C$. Interestingly, the data for the major products (propane, n-butane, and isopentane) now differed only slightly for the mordenites and the Y-zeolites despite the variation in reaction temperature, the large difference in acidity and activity, and the much longer chain length with the former.

At constant temperature an increasing conversion will increase the partial pressure of all intermediate species. This should lead to a higher probability for secondary reactions and this factor could be at least partly responsible for the changing product distributions as a function of conversion. In Tables 4 and 5, results obtained on different H−Y zeolites and mordenites at identical temperature and overall conversions were collected. Interestingly, large increases in TOF with increasing Si/Al were observed, but without significant change in selectivity. A fourfold increase in overall TOF over H−Y zeolites resulted in a 14% change in chain length only.

TABLE 4

TOF of Isobutane Conversion on H−Y Zeolites at 370°C, 2.3% Overall Conversion[a]

Catalyst	LZ–210(6)[0.1]	LZ–210(9)[0.1]	LZ–210(12)[0.1]	LZ–Y82
H_2	1.1	2.0	2.3	4.0
CH_4	1.0	2.2	2.3	4.5
C_2H_6	0.0	0.0	0.0	0.0
C_2H_4	0.1	0.1	0.2	0.3
C_3H_8	2.3	7.1	7.7	14.1
C_3H_6	0.8	0.8	1.0	1.7
n-C_4H_{10}	12.2	30.7	31.9	59.1
i-C_4H_8	1.4	1.6	1.9	3.6
n-C_4H_8	0.8	1.1	1.2	2.4
i-C_5H_{12}	2.8	5.7	6.5	11.2
n-C_5H_{12}	0.0	0.0	0.0	0.0
$H_2 + CH_4$	2.1	4.2	4.6	8.5
Σ_3^5 alkanes	17.3	43.5	46.1	84.4
Conv.$(A)^b$	19.4	47.7	50.7	92.9
Conv.$(B)^c$	20.5	47.1	50.3	92.2
$C_4/(C_3 + C_5)^d$	2.4	2.4	2.2	2.3
C_3/C_5^d	0.8	1.2	1.2	1.3
% initiation^e	12.1	9.7	10.0	10.1
Chain length^f	8.2	10.4	10.0	9.9
% conv.(B)	2.3	2.3	2.3	2.3

^{a} TOF is given as 10^{-6} molec. Al_F^{-1} s^{-1}; 400 mg of catalyst was used; $F/W = 1.1 \times 10^{-5}$ mol $g^{-1}s^{-1}$.
^{b}Conversion$(A) = (H_2 + CH_4) + \Sigma_3^5$ alkanes.
^{c} Conversion$(B) = 1/4 \; \Sigma_1^5 jC_i$, where j is the number of carbon atoms in each of the i products.
^{d} Ratio of alkanes.
^{e} % initiation reaction $= [(H_2 + CH_4)/Conv.(A)] \times 100$.
^{f} Σ_1^3 alkanes/$(H_2 + CH_4)$; i.e., the number of isobutane molecules reacted by hydride or alkyde transfer for every chain initiated by Brønsted acid sites.

TABLE 5

TOF of Isobutane Conversion on H−Mordenites at 250°C, 2.3% Overall Conversion[a]

Catalyst	JRC–Z–HM10	JRC–Z–HM15	JRC–Z–HM20	LZ–M8
H_2	0.3	0.4	0.5	0.4
CH_4	0.2	0.3	0.3	0.3
C_2H_6	0.0	0.0	0.0	0.0
C_2H_4	0.0	0.0	0.0	0.0
C_3H_8	16.2	23.3	30.3	26.3
C_3H_6	0.0	0.0	0.0	0.0
n-C_4H_{10}	58.6	84.5	100.2	95.6
i-C_4H_8	0.0	0.0	0.0	0.0
n-C_4H_8	0.0	0.0	0.0	0.0
i-C_5H_{12}	14.5	20.8	27.5	23.8
n-C_5H_{12}	1.6	2.3	2.7	2.4
$H_2 + CH_4$	0.5	0.7	0.8	0.7
Σ_3^5 alkanes	90.9	130.9	160.8	148.1
Conv.$(A)^b$	91.4	131.6	161.5	148.8
Conv.$(B)^c$	90.9	130.9	160.8	148.2
$C_4/(C_3 + C_5)^d$	1.8	1.8	1.7	1.8
C_3/C_5^d	1.0	1.0	1.0	1.0
% primary^e	0.6	0.5	0.5	0.5
Chain length^f	182.0	187.0	201.0	212.0
% conv.(B)	2.3	2.3	2.3	2.3

^{a} TOF is given as 10^{-6} molec. Al_F^{-1} s^{-1}; 400 mg of catalyst was used; $F/W = 1.1 \times 10^{-5}$ mol $g^{-1}s^{-1}$.
^{b}Conversion$(A) = (H_2 + CH_4) + \Sigma_3^5$ alkanes.
^{c} Conversion$(B) = 1/4 \; \Sigma_1^5 jC_i$, where j is the number of carbon atoms in each of the i products.
^{d} Ratio of alkanes.
^{e} % Primary reaction $= [(H_2 + CH_4)/Conv.(A)] \times 100$.
^{f} Σ_3^5 alkanes/$(H_2 + CH_4)$; i.e., the number of isobutane molecules reacted by hydride or alkyde transfer for every chain initiated by Brønsted acid sites.

The TOFs of hydrogen and methane formation over LZ–Y82 at three temperatures are plotted vs the partial pressure of isobutane (6.3, 10.0, and 17%) in the feed in Fig. 5A. Clearly, a first order dependence in isobutane pressure was obtained. The related results for the alkane products formed in the carbenium chain processes are presented in Fig. 5B, where a good second-order dependence was obtained, confirming the results of McVicker *et al.* (2).

Reactions of n-butane. Some experiments were also carried out under comparable conditions using n-butane as a feed. Four catalysts were tested: LZ–Y82 and LZ–210(9)[0.1] at 370°C, LZ–M8 and JRC–Z–HM15 at 250 and 300°C. TOFs for product formation are given for LZ–Y82 and LZ–M8 in Table 6. The reactions of the two isomers were quite similar in character, although the total conversion of isobutane was faster (on mordenite about three times) than that of n-butane. As in the case of isobutane, the isomerization product was the largest single product. Propane formed in large excess to pentane.
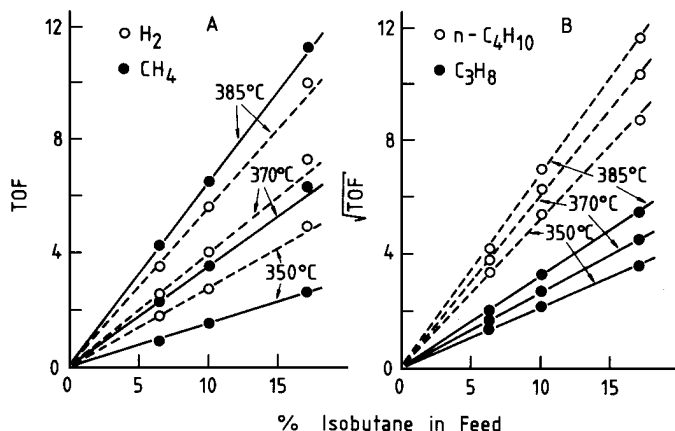
FIG. 5. (A) TOF [(mol $Al_F^{-1}s^{-1}$) $\times 10^{-6}$] of H_2 (○) and CH_4 (●) formation; (B) $\sqrt{TOF}$ [(mol $Al_F^{-1}s^{-1})^{1\backslash2} \times 10^{-3}$] of n-butane (○) and propane (●) formation of LZ–Y82 as a function of isobutane concentration in the feed; 400 mg of catalyst was used; experiments with different concentration of isobutane were carried out independently; the temperature was varied randomly up and down.

It has previously been demonstrated (20, 21) that n-butane cracking may be initiated by protonation of either a primary carbon resulting in the formation of hydrogen and butene or a secondary carbon resulting in the formation of methane + propene and ethane + ethylene. In Fig. 6, the results of experiments with varying feed rates of n-butane (constant weight of catalyst) are presented. The experiments were carried out at 370°C over Y-zeolites and at 250°C over mordenites. These plots of yields of hydrogen, methane, ethane, and ethylene vs total conversion had characteristics similar to those obtained for the initial products of isobutane conversion (Figs. 2–4). For each product, points for two catalysts fell on the same curves, although these were different for H–M and H–Y. From the shape of these curves it can be concluded that, like hydrogen and methane from isobutane, each of these compounds was produced in the primary protonolysis of n-butane. As with isobutane, the yields of these products at identical conversions were much lower over mordenites than over H–Y zeolites because of the much longer chain lengths. Over mordenites the yields of ethane and ethylene were identical within the experimental error and extremely low at 250°C; the yields increased in the sequence of $C_2 < H_2 < CH_4$.

Addition of alkenes. On mordenites, the yield of initial products and consequently the yield of alkenes were extremely low compared to the yield of alkanes from both *iso*- and n-butane as reactant. The effect of alkenes on the cracking were studied on LZ–M8 by addition of small amounts of alkenes to the feed (alkene/butane = 0.01). Without this addition, the rate of propane, pentane, and butane isomer formation was almost constant during 170 min on stream (Figs. 7 and 8). Ethylene, propene, and i-butene additives resulted in a large increase in the rates of alkane formation.

TABLE 6

TOF of n-Butane Conversion on LZ–Y82 at 370°C and on LZ–M8 at 300°C[a]

Catalyst	LZ–Y82	LZ–M8
H_2	1.5	6.9
CH_4	3.5	3.5
C_2H_6	3.0	7.4
C_2H_4	2.7	3.0
C_3H_8	3.7	35.5
C_3H_6	0.5	0.7
i-C_4H_{10}	20.6	125.8
i-C_4H_8	1.7	0.0
n-C_4H_8	1.0	4.0
i-C_5H_{12}	0.0	12.7
n-C_5H_{12}	0.0	6.2
$H_2 + CH_4 + C_2H_6$	8.0	17.8
Σ_3^5alkanes	24.3	180.2
Conv.(A)[b]	32.3	198.0
Conv.(B)[c]	30.3	183.4
$C_4/(C_3 + C_5)$[d]	5.5	2.3
C_3/C_5[d]	—	1.9
% initiation[e]	24.8	9.0
% conv.(B)	0.2	1.2

[a] TOF is given as 10^{-6} molec. Al_F^{-1} s^{-1}; 400 mg of catalyst was used; $F/W = 1.1 \times 10^{-5}$ mol g^{-1}s^{-1}.
[b] Conversion$(A) = (H_2 + CH_4) + C_2H_6 + \Sigma_3^5$ alkanes.
[c] Conversion$(B) = 1/4 \ \Sigma_1^5 jC_i$, where j is the number of carbon atoms in each of the i products.
[d] Ratio of alkanes.
[e] % initiation reaction $= [(H_2 + CH_4 + C_2H_6)/Conv.(A)] \times 100$.

The rates, however, dropped continuously with time on stream (TOS). The rates of individual alkanes were affected in different ways by the different alkenes.

The enhancement of propane formation from both *iso*- and n-butane increased in the sequence of ethylene < i-butene < propene. The alkenes, especially propene, had a longer lasting effect on the rate of propane formation than
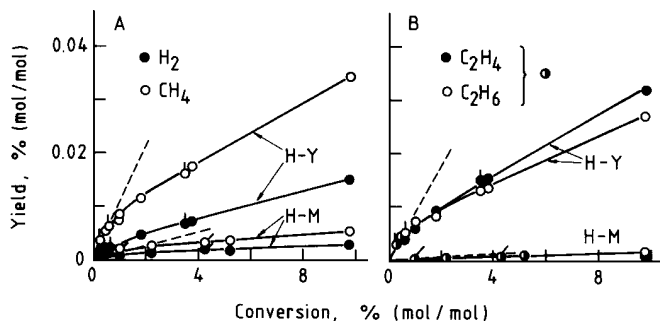

FIG. 6. Yield of (A) hydrogen (●) and methane (○) and, (B) ethylene (●) and ethane (○) as a function of total n-butane conversion over LZ–210(9)[0.1] and LZ–Y82 (flagged) at 370°C as well as over JRC–HM15 and LZ–M8 (flagged) at 250°C; 400 mg of catalyst was used; F/W was varied between 1.1×10^{-5} and 1.8×10^{-6} moles g^{-1}s^{-1} from the higher to lower values.
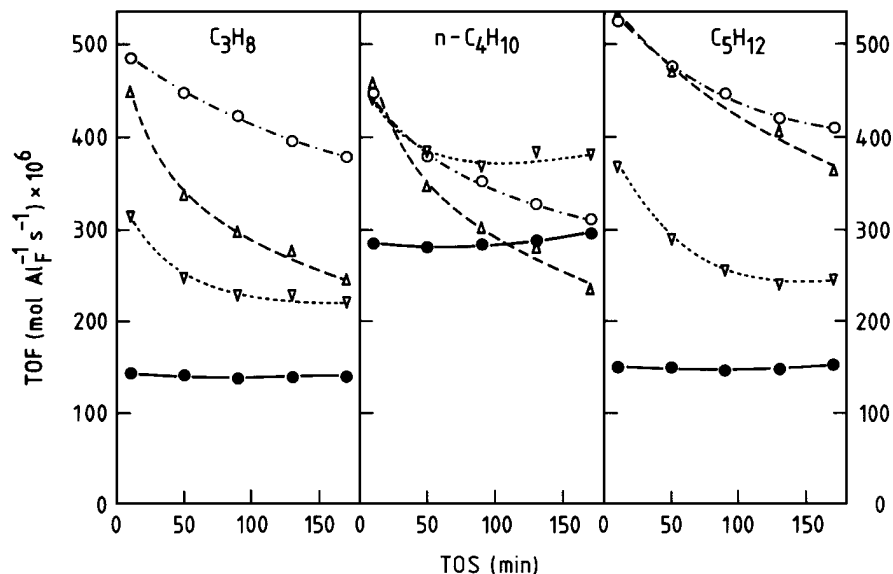
FIG. 7. TOF of propane, isobutane, and pentane formation from isobutane on LZ–M8 at 300°C with different alkenes in the feed as a function of TOS; (∇) ethylene, ($\circ$) propene, ($\triangle$) i-butene, ($\bullet$) none in the feed; 400 mg of catalyst was used; F/W was 1.1×10^{-5} moles $g^{-1}s^{-1}$ for isobutane and 1.1×10^{-7} moles $g^{-1}s^{-1}$ for alkenes.

on isomerization. Formation of pentane was identically enhanced by propene and i-butene. However, from n-butane the rate of pentane formation (Fig. 8) was significantly lower than the rates of propane formation and isomerization, while from isobutane the rate of pentane formation surpassed both of them in the presence of propene and i-butene (Fig. 7).

Interestingly, at low TOS, the three alkenes had an identical effect on the rate of n-butane formation from isobu-

tane (Fig. 7) but the drop in the rate with TOS increased in the sequence of ethylene < propene < i-butene. The alkenes had almost mirrored effect on the rate of n-butane isomerization (Fig. 8). At low TOS, the enhancement increased in the sequence of ethylene < propene < i-butene, but after 170 min the rates were almost the same as without alkene additives.

It is interesting to note that the consumption of propene and i-butene (Fig. 9) was significantly lower than the
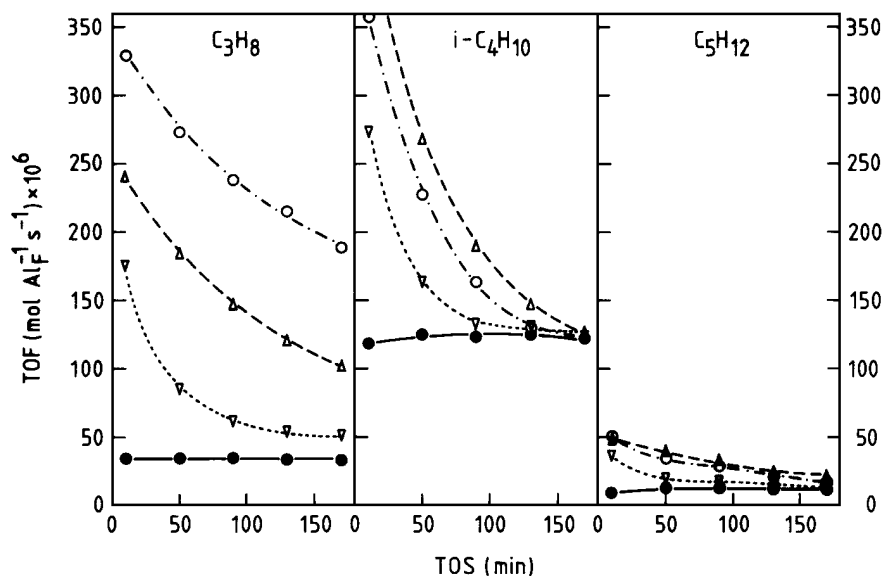

FIG. 8. TOF of propane, isobutane, and pentane formation from n-butane on LZ–M8 at 300°C with different alkenes in the feed as a function of TOS; (∇) ethylene, ($\circ$) propene, ($\triangle$) i-butene, ($\bullet$) none in the feed; 400 mg of catalyst was used; F/W was 1.1×10^{-5} moles $g^{-1}s^{-1}$ for n-butane and 1.1×10^{-7} moles $g^{-1}s^{-1}$ for alkenes.
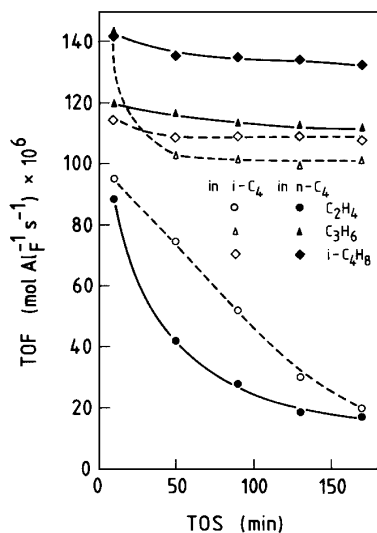
FIG. 9. TOF of alkene consumption from *iso*- and *n*-butane on LZ–M8 at 300°C as a function of TOS; for details see Figs. 7 and 8.

excess of propane and isomerization products that resulted by enhancement. After the initial drop, consumption remained almost constant during 170 min; the consumption of ethylene, however, dropped almost to zero during this period.

DISCUSSION

Relatively little work has been published concerning the reaction of butanes over mordenites. Bearez *et al.* (23) found that the rate of isobutane transformation was twice that of *n*-butane; a factor of about three was obtained in the present work (compare Tables 3 and 6) and a factor of two for LZ–Y82 (Tables 2 and 6). They concluded that propane and pentane were formed by disproportionation of butanes, although the propane to pentane ratio varied significantly with TOS.

Krupina *et al.* (24, 25) reported that isomerization of *n*-butane over mordenites resembled that in strong liquid acids; i.e., it is accompanied by cracking and disproportionation reactions. They suggested that the latter processes proceeded via an intermediate of carbocation formed in alkylation by alkenes. They found that the rates of cracking and disproportion could be influenced more significantly by the carbocation population than the rate of isomerization.

Maness and Dooley (26) found that addition of 0.2% isobutene to *n*-butane increased the conversion on mordenite significantly. Product distributions in reactions of butanes were similar to product distributions obtained with solid superacids. In turn, the criteria for superacidity is frequently drawn from the fact that a certain catalyst was found to be active in isomerization of *n*-butane. Previous results (12) suggested that mordenite contains sites with the strength of superacids.

The close resemblance of the product distribution as a function of conversion on mordenites (Fig. 4) and Y-zeolites (Figs. 2 and 3) suggests that the same general processes are occuring with both types of zeolite. Note, however, that an approximately 10-fold higher rate of initiation is required with Y-zeolites to reach an identical conversion with mordenites.

According to Dwyer and co-workers (14), in conversion of isobutane over H–ZSM-5 catalysts, the shape of the curve for the yield of methane as a function of conversion depends on the reaction temperature. As the temperature is lowered, the length of the initial linear section of plots decreased followed by a section with a lower slope. Normally, the declining slope of this curve is indicative of secondary reactions of the particular product. In the case, when methane is formed in the initiation reaction, there is no apparent way it can be consumed in a secondary reaction. Here the change in slope indicates a change in the rate of methane formation or a change in the mechanism responsible for its production. Similar characteristics for these initiation products of isobutane (Figs. 2–4) and *n*-butane. (Fig. 6) conversion were observed by us. The slopes of the plots decreased with increasing conversion. This may result if the initiation mechanism becomes less significant compared to the secondary carbenium ion chain process. At higher conversion the chain length increases and the contribution of primary products to the total conversion becomes negligible, especially with mordenites.

A remarkable feature of Figs. 2–4 is that in each case all the data for different catalysts fell on the same curves. This suggests that product distribution on catalysts with identical structure is governed mainly by the temperature and the total conversion. The effective contact time was controlled by the number of active sites (Si/Al ratio, Figs. 2 and 4), by poisoning a fraction of sites (e.g., by sodium, Fig. 3) or by varying the feed rate. The yield of individual product at a given temperature is a function of the conversion and consequently of the contact time. This explains why the chain length on different catalysts but at identical temperature and conversion is almost identical (Tables 4 and 5).

Recently Wojciechowski and co-workers (18) concluded that the pathways for isomerization and cracking of alkanes are not independent. They are alternative events in the conversion of feed by a chain reaction mechanism. According to Rice and Wojciechowski (27) the total activity of the catalyst changes with TOS as the population of carbenium ions varies due to desorption and readsorption of products.

Following a suggestion by Haag and Dessau (28), Hall and co-workers (4–11) suggested that the most likely way to initiate the conversion of isobutane on Y-zeolites is the protonation on Brønsted acid sites (Eq. [1]). Protonation of C–H or C–C bonds produces pentacoordinated transition states which are not stable and decompose to form hydrogen or methane and the more stable *t*-butyl and *i*-propyl

carbenium ions. Relative rates of protonation on C−C and C−H bonds and decomposition via different routes depend on the conditions, most defining among which are the temperature and the strength of sites. As can be seen in Fig. 5, at lower temperature dehydrogenation is preferred, while at higher temperature demethanation becomes more important.

At low conversion, when the surface sites are populated mainly with the corresponding carbenium ions, it is most probable that isomerization occurs followed by H-transfer from the feed isobutane. Thus chain propagation results from these processes. According to Marczewski (19), carbenium ions may also attack C−H and C−C bonds of alkane molecules forming pentacoordinated transition complexes, which decompose with the result of hydride or methyl transfer to the carbenium ion. Interestingly, carbenium ions formed on Brønsted acid centers may be regarded as Lewis acid sites and the hydride or methyl transfer as H$^-$ or CH$_3^-$ abstraction by this Lewis acid. In this way, propane (and t-butyl carbenium ion) is formed in hydride transfer between isobutane and propyl carbenium ion. Isopentane (and propyl carbenium ion) is formed in methyl transfer between isobutane and sec-butyl carbenium ions. Hydride transfer between isobutane and t-butyl carbenium ion, and methyl transfer between isobutane and the i-propyl ion are degenerate processes. These can explain why propane and pentanes are not formed in strictly 1 : 1 ratio.

Methyl transfer between isobutane and $tert$- or sec-butyl carbenium ion should provide neopentane or isopentane, respectively. Formation of neopentane was not observed on zeolites but was on fluorided alumina (11), which contains less narrow pores than zeolites. Monomolecular isomerization of t-butyl followed by hydride transfer to sec-butyl carbenium ion leads to the formation of n-butane. Methyl transfer to n-propyl ion should not be very important because of the relative instability of the primary carbenium ion.

Addition of alkenes enhanced the conversion of isobutane (Fig. 7). Propene and i-butene can be protonated more easily than isobutane; therefore, the carbenium ion concentration is much higher than with isobutane alone. As discussed above, chain propagation may proceed by hydride and methyl abstraction from isobutane. Comparing Figs. 7 and 9, we can see that the growth in the yield of propane and pentane is higher than the consumption of propene and i-butene. This is to be expected if the chain length is higher than unity.

The effect of ethylene on the conversion of isobutane requires some further consideration. The rate of ethane formation increases insignificantly by addition of ethylene. This shows the low participation of ethyl carbenium ion in the hydride transfer process. The majority of ethylene presumably took part in dimerization or oligomerization. The rate of ethylene consumption dropped with TOS (Fig. 9),

indicating that the sites available for ethylene oligomerization decreases due to precoke deposition.

In conversion of isobutane alone, the yield of primary products and consequently the yield of alkenes was extremely low on mordenites (Fig. 4). Thus the activity remained constant (Fig. 7). Addition of alkenes to the feed enhanced the activity but at the same time increased the rate of deactivation. Presumably, like ethylene, a fraction of propene and isobutene takes part in oligomerization; this contributes to the catalyst deactivation. Similarly, when the conversion of isobutane was carried out at higher temperature, the yield of initiation products and thus alkenes was higher. Now steady-state conditions could not be attained due to continuous deactivation.

In the conversion of n-butane, besides hydrogen a butyl carbenium ion and methane together with a propyl carbenium ion were primary initiation products as were ethane and ethylene (Fig. 6), as expected from a protolytic attack on the middle C−C bond of n-butane. Gates and co-workers (20–22) showed that on H–ZSM-5 all three of these products were formed at approximately the same rate and had about the same activation energy. On the contrary, on H−Y zeolites at 370°C the rates extrapolated to zero conversion varied in the sequence of CH$_4 \sim$ C$_2$H$_6 >$ H$_2$, while on mordenite at 250°C this order is CH$_4 >$ H$_2 >$ C$_2$H$_6$. The ratio of initial rates seems to be a function of temperature as in the case of isobutane (Fig. 5).

Interestingly the ratio of propane to pentane formed from isobutane was close to the unity (Fig. 7); from n-butane, however, significantly more propane than pentane was formed (Fig. 8). This observation is in contradiction to the hypothesis that propane and pentane were formed by disproportionation, in disruption of a C$_8$ intermediate. It seems more probable that the mechanism for hydride and methyl transfer to carbenium ions described above is the effective process. Methyl transfer from isobutane takes place more easily than from n-butane, which explains the hindered formation of pentane from the latter.

A tendentious difference was observed in the ratio of iso- to n-pentane formed on mordenite under identical conditions from iso- and n-butane. As an average of several experimental data, this ratio is 16 for isobutane and only 1.6 for n-butane. This shows to the preferential formation of pentanes with identical structure as the parent butane. The difference may arise from the chemical processes allowable from the different carbenium ion population characteristic for the two butane isomers.

As can be seen in Figs. 7 and 8, when alkenes were added to butanes, the product composition varied significantly with TOS. The variation of the concentration of different carbenium ions is a prerequisite of this process. As described by Rice and Wojciechowski (27), the active sites of the catalysts need not be the sites present on the inorganic framework of the original catalyst, but rather consists

of carbenium ions residing on the original sites. Each carbenium ion on the catalyst will present a certain level of activity toward feed. The levels of activity vary with increasing coke formation. Consequently there is not only a general tendency for decreasing conversion with TOS, but the lifetime (steady-state concentration) of different carbenium ions varies in different ways.

REFERENCES

1. McVicker, G. B., Kramer, G. M., and Ziemiak, J. J., *J. Catal.* **83**, 286 (1983).
2. McVicker, G. B., Kramer, G. M., and Ziemiak, J. J., *J. Catal.* **92**, 355 (1985).
3. Beyerlein, R. A., McVicker, G. B., Yacullo, L. M., and Ziemiak, J. J., *J. Phys. Chem.* **92**, 1967 (1988).
4. Lombardo, E. A., Pierantozzi, R., and Hall, W. K., *J. Catal.* **110**, 171 (1988).
5. Lombardo, E. A., Gaffney, T. R., and Hall, W. K., *in* "Proceedings, 9th International Congress on Catalysis, Calgary, 1988" (M. J. Phillips and M. Ternan, Eds.), Vol. 1, p. 412. Chem. Institute of Canada, Ottawa, 1988.
6. Lombardo, E. A., and Hall, W. K., *J. Catal.* **112**, 565 (1988).
7. Lombardo, E. A., Sill, G. A., and Hall, W. K., *J. Catal.* **119**, 426 (1989).
8. Shertukde, P. V., Marcelin, G., Sill, G. A., and Hall, W. K., *J. Catal.* **139**, 468 (1993).
9. Hall, W. K., Engelhardt, J., and Sill, G. A., *in* "Zeolites: Facts, Figures, Future" (P. A. Jacobs and R. A. van Santen, Eds.), p. 1253. Elsevier, Amsterdam, 1989.
10. Engelhardt, J., and Hall, W. K., *J. Catal.* **125**, 472 (1990).
11. Engelhardt, J., and Hall, W. K., *J. Catal.* **157**, 721 (1995).
12. Umansky, B., Engelhardt, J., and Hall, W. K., *J. Catal.* **127**, 128 (1991).
13. Stefanadis, C., Gates, B. C., and Haag, W. O., *J. Molec. Catal.* **67**, 363 (1991).
14. Shigeishi, R., Garforth, A., Harris, I., and Dwyer, J., *J. Catal.* **130**, 423 (1991).
15. Olah, G., Halpern, V., Shen, J., and Mo, Y. K., *J. Amer. Chem. Soc.* **93**, 1251 (1971).
16. Olah, G. A., and Lin, H. C., *J. Amer. Chem. Soc.* **93**, 1256 (1971).
17. Olah, G. A., Surya Prakash, G. K., and Sommer, J., "Superacid," p. 244. Wiley, New York, 1985.
18. Zhao, Y., Bamwenda, G. R., Groten, W. A., and Wojciechowski, B. W., *J. Catal.* **140**, 243 (1993).
19. Marczewski, M., *J. Chem. Soc., Faraday Trans. I.* **82**, 1687 (1986).
20. Fuentes, G. A., Boegel, J. V., and Gates, B. C., *J. Catal.* **78**, 436 (1982).
21. Fuentes, G. A., and Gates, B. C., *J. Catal.* **76**, 440 (1982).
22. Kranilla, H., Haag, W. O., and Gates, B. C., *J. Catal.* **135**, 115 (1992).
23. Bearez, C., Chevalier, F., and Guisnet, M., *React. Kinet. Catal. Lett.* **22**, 405 (1983).
24. Krupina, N. N., Dorogochinskii, A. Z., Meged, N. F., and Schmailova, V. I., *React. Kinet. Catal. Lett.* **23**, 273 (1983).
25. Krupina, N. N., Proskurnin, A. L., and Dorogochinskii, A. Z., *React. Kinet. Catal. Lett.* **32**, 135 (1986).
26. Maness, J. A. Jr., and Dooley, K. M., *J. Catal.* **117**, 322 (1989).
27. Rice, N. M., and Wojciechowski, B. W., *Canad. J. Chem. Eng.* **69**, 1100 (1991).
28. Haag, W. O., and Dessau, R. M., *in* "Proceedings 8th International Congress on Catalysis, Berlin, 1984," Vol. 2, p. 305. Dechema, Frankfurt-am-Main, 1984.